

FoNE: Precise Single-Token Number Embeddings via Fourier Features

Tianyi Zhou Deqing Fu Mahdi Soltanolkotabi Robin Jia Vatsal Sharan

Department of Computer Science
University of Southern California
Los Angeles, CA 90089

{tzhou029,deqingfu,soltanol,robinjia,vsharan}@usc.edu

Abstract

Large Language Models (LLMs) typically represent numbers using multiple tokens, which requires the model to aggregate these tokens to interpret numerical values. This fragmentation makes both training and inference less efficient and adversely affects the model’s performance on number-related tasks. Inspired by the observation that pre-trained LLMs internally learn Fourier-like features for number tokens, we propose **Fourier Number Embedding (FoNE)**, a novel method that directly maps numbers into the embedding space with their Fourier features. FoNE encodes each number as a single token with only two embedding dimensions per digit, effectively capturing numerical values without fragmentation. This compact representation accelerates both training and inference. Compared to traditional subword and digit-wise embeddings, FoNE not only reduces computational overhead but also achieves higher accuracy across various numerical tasks including addition, subtraction and multiplication. On 6-digit decimal addition, FoNE requires $64\times$ less data to achieve 99% accuracy than subword and digit-wise embeddings while using $3\times$ and $6\times$ fewer tokens per number, respectively. Furthermore, FoNE is the only method that yields 100% accuracy on over 100,000 test examples for addition, subtraction, and multiplication. The codes and visualization are available at <https://fouriernumber.github.io/>.

1 Introduction

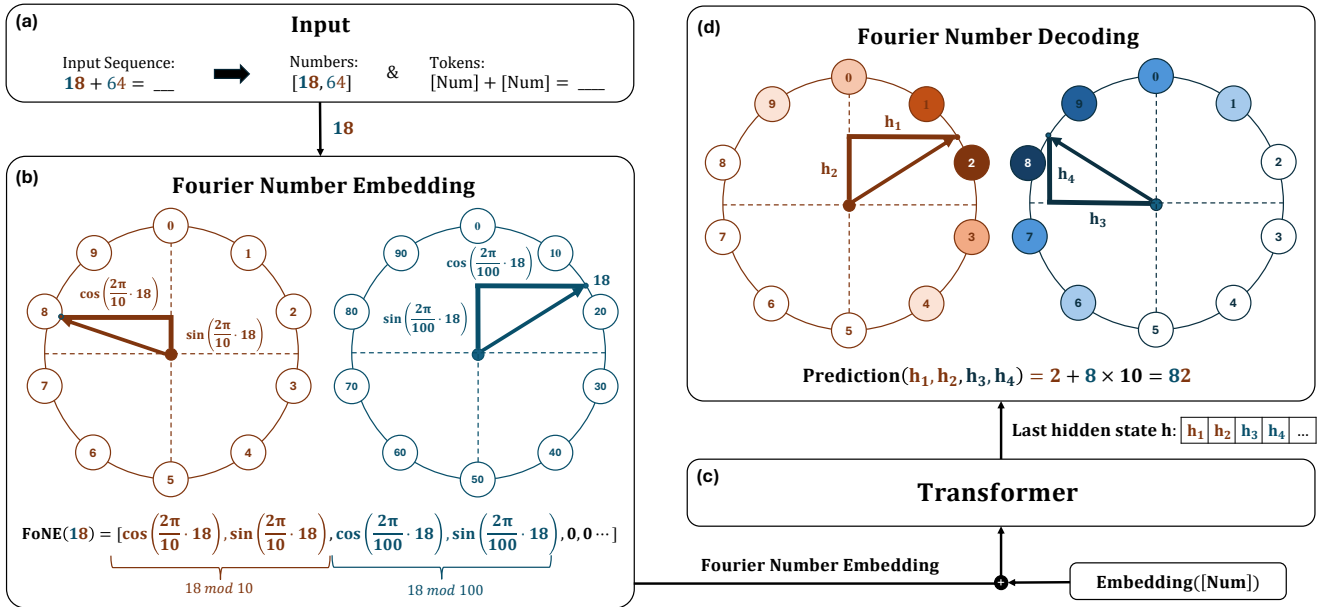


Figure 1: (a) We extract all the numbers from the input sequence. (b) For each number, we use FoNE to directly map the number to its embedding. The first two entries in the embedding represent $18 \bmod 10$, while the next two entries represent $18 \bmod 100$. (c) We pad the FoNE with zeros, add it to the word embeddings, and then feed the combined embeddings into the model. (d) For each digit, we take every two entries from the last hidden state and find the number whose representation is closest to these two entries.

Large language models (LLMs) require precise representations of numerical data to perform number-related tasks effectively. However, since LLMs treat numbers just like any other token, embeddings of numerical tokens do not systematically capture important numerical features. As a result, it is challenging for even billion-parameter models to achieve perfect accuracy in solving simple arithmetic tasks [37, 7, 20, 38, 47].

While generating code can be a useful workaround, relying solely on this capability highlights a fundamental limitation: without a proper understanding of numbers, the model cannot fully grasp concepts critical to domains like mathematical theorems, physics laws, or quantitative reasoning. Even with approaches like Chain-of-Thought (CoT) prompting, it is important to have a perfect accuracy in solving basic arithmetic tasks to build a strong foundation for more complex reasoning.

Standard tokenization approaches, such as subword tokenization (e.g., GPT-4o [2], Llama-3 [6], Phi-2 [1]) or digit-wise tokenization (e.g., Llama-2 [44], Mistral [16]), force the model to aggregate multiple tokens to understand numbers and introduces inefficiencies by tokenizing one number to multiple tokens. However, this inefficiency in tokenizing numbers leads to larger challenges when it comes to their representation. Numbers, unlike words, require systematic, frequency-agnostic representations, yet LLMs often exhibit a frequency bias in arithmetic tasks [35], predicting numbers based on training data prevalence rather than adhering to their mathematical properties.

We draw inspiration from interpretability analyses of LLMs, which reveal that models internally develop Fourier-like features. Specifically, pre-trained models embed number tokens using a sparse set of features in the Fourier domain [49]. These features enable the representation of numbers capturing both the magnitude and exact values of numbers, which are critical for solving arithmetic tasks [49]. However, due to limitations in sub-word tokenization, current LLMs struggle to extend this mechanism to larger

numbers, highlighting the need for more systematic approaches for numerical representation.

In this paper, we propose a novel approach called Fourier Number Embedding (FoNE), which directly maps numbers into their Fourier representations, bypassing the tokenization step entirely. By representing each digit using *cosine and sine functions with different periods*, as shown in Figure 1(b), FoNE ensures precise representation of numbers. This approach encodes the modular relationship of each digit through periodic functions, enabling recovery of $x \bmod 10^i$ for all digits i . Note that, for FoNE, each digit is represented using only two dimensions in the embedding vector. This compact design not only reduces computational overhead but also creates opportunities for future extensions by incorporating additional features to better capture numeric properties. By embedding and predicting numbers directly as single tokens, our method eliminates the need for multiple forward passes and token aggregation, significantly enhancing computational efficiency. Furthermore, we provide a theoretical justification for why FoNE can represent numbers accurately as single tokens, leveraging the modular encoding properties of trigonometric functions to ensure exact recovery of each digit through periodic embeddings.

Beyond theoretical justifications, we demonstrate the effectiveness of FoNE through extensive experiments on a range of arithmetic tasks, including addition, subtraction, and multiplication. Our results show that FoNE is the only approach that can achieve perfect accuracy on multiple arithmetic tasks while requiring significantly less training data and fewer model parameters compared to existing methods. Moreover, FoNE offers faster training and inference times by encoding each number into a single token, thereby reducing the computational overhead. These findings underscore FoNE’s capacity to represent and manipulate numerical data both efficiently and precisely within large language models.

2 Related Work

Arithmetic and Number-Related Tasks in LLMs. Addressing number-related tasks through next-token prediction remains a significant challenge, such as arithmetic [37, 46, 26], time-series prediction [41, 28, 23, 48, 21, 18], quantitative reasoning [25, 22, 4, 19, 5], and handling tabular data [11, 8, 36]. Despite advancements in transformer-based models, LLMs such as GPT-3 and GPT-4, with billions of parameters, struggle to solve simple arithmetic problems involving multi-digit addition and multiplication across multiple forward passes [7, 9], even when using scratchpads [31].

Lee et al. [20] demonstrate that smaller transformer models can successfully handle multiplication when equipped with carefully designed scratchpads. Other approaches, such as those proposed by Golkar et al. [13], Sundararaman et al. [40], Jiang et al. [17], Sivakumar and Moosavi [39], introduce number embedding methods to enhance model performance on number-related tasks. However, the range of numbers these methods can accurately represent is typically limited to fewer than five digits. Additionally, a line of research [24, 38] incorporates the positional information of digits into embeddings or adds it as extra tokens [30]. Zhou et al. [50] shows that digit-wise tokenization is better than subword tokenization. Thawani et al. [43] explores encoding strategies like digit-by-digit, scientific notation, and base-10 formats, while Jiang et al. [17] maps numbers to finite “prototype numerals.” These methods help the model align digits of equal significance but often require digit-wise tokenization or introduce additional tokens, reducing training and prediction efficiency. In contrast, the method proposed in this paper precisely encodes all numbers as a single token, eliminating range limitations and avoiding the efficiency drawbacks associated with previous approaches.

Fourier Features. Fourier features are commonly observed in image models, particularly in the early layers of vision models [33, 32, 10]. These features enable the model to detect edges, textures, and other spatial patterns effectively. However, Transformers struggle to capture high-frequency components in [3, 42]. Augmenting data with high-frequency components or explicitly encoding coordinates using Fourier features has been demonstrated to improve model performance [42, 15]. In modular addition tasks, studies have revealed that after “grokking”, a one-layer Transformer can learn to solve the task

perfectly by leveraging Fourier features [29, 14]. Furthermore, Zhou et al. [49] demonstrates that LLMs naturally encode numbers using Fourier features during pretraining, leveraging these representations for arithmetic tasks. Building on this insight, we propose encoding numbers precisely through Fourier features by representing residues in various modular groups, enabling algebraic operations to be performed in a component-wise, parallel manner.

3 Methods

Building on insights from prior studies [49] that highlight the importance of Fourier features in numerical embeddings, we propose Fourier Number Embedding. Unlike existing methods that often require digit-wise tokenization or pre-training to handle numeric tasks, FoNE directly maps numbers into compact Fourier representations.

In Section 3.1, we introduce FoNE, where each digit is represented with two entries in their embeddings. In Section 3.2, we introduce the Fourier number loss function and Fourier number prediction, which demonstrate how we decode the last hidden states from Fourier space to number space to compute loss and make the prediction. In Section 3.3 we show how we incorporate our method into input sequences. The complete process is shown in Figure 1.

3.1 Fourier Number Embedding (FoNE)

Algorithm 1 Fourier Number Embedding (FoNE) Algorithm

```

1: procedure FOURIERNUMBEREMBEDDING( $x \in \mathbb{R}, m \in \mathbb{Z}_{\geq 0}, n \in \mathbb{Z}_{\geq 0}, d \in \mathbb{Z}_{>0}$ )
2:   Inputs: Number  $x$ , integer digit length  $m$ , decimal digit length  $n$ , embedding dimension  $d$ 
3:   Initialize empty embedding vector FoNE  $\leftarrow []$ 
4:   for  $i = -n + 1 \rightarrow m$  do                                      $\triangleright$  Loop over all scales from  $10^{-n+1}$  to  $10^m$ 
5:      $T_i \leftarrow 10^i$                                             $\triangleright$  Set the period for the current scale
6:      $\phi(x, T_i) \leftarrow (\cos(\frac{2\pi}{T_i}x), \sin(\frac{2\pi}{T_i}x))$         $\triangleright$  Compute the circular embedding for scale  $T_i$ 
7:     Append  $\phi(x, T_i)$  to FoNE                                      $\triangleright$  Add the embedding for this scale to the result
8:   end for
9:   while Length(FoNE) <  $d$  do                                      $\triangleright$  Ensure embedding dimension matches the target
10:    Append 0 to FoNE                                                $\triangleright$  Zero-pad
11:  end while
12:  return FoNE
13: end procedure

```

We first introduce the following circular embedding function that maps each $x \in \mathbb{R}$ to a point on the unit circle.

Definition 3.1 (Circular embedding). *Let T be a given period. We define function $\phi : \mathbb{R} \rightarrow \mathbb{R}^2$*

$$\phi(x, T) := (\cos(\frac{2\pi}{T}x), \sin(\frac{2\pi}{T}x)).$$

Let m represents the number of digits before the decimal point, and n represents the number of digits after the decimal point, ensuring that both integer and fractional parts of a number are accounted for in the representation. Next, we formally define the FoNE method that directly map numbers to their embedding.

Definition 3.2 (Fourier Number Embedding). *Let m be the integer digit length, and n be the decimal digit length. We define the Fourier Number Embedding function FoNE : $\mathbb{R} \rightarrow \mathbb{R}^{2(m+n)}$ for an input number x as follows:*

$$\text{FoNE}(x, m, n) := [\phi(x, T_i)]_{i=-n+1}^m,$$

where $T_i = 10^i$ for each integer i in the range $-n + 1$ to m .

To align the embedding dimensions of FoNE with the model’s input embedding dimension d , we map the Fourier Number Embedding, which lies in $\mathbb{R}^{2(m+n)}$, to \mathbb{R}^d . This mapping can be achieved in two ways: (1) by applying a learnable linear transformation $\mathbf{W} \in \mathbb{R}^{d \times 2(m+n)}$, or (2) by appending zeros to the embedding vector to match the dimensionality d . As demonstrated in Section 4.3, both approaches achieve comparable results.

Then, we introduce an elementary lemma and demonstrate why FoNE can preserve the numeracy on numbers.

Lemma 3.3 (Informal version of Lemma C.1). *Given the pair $(\cos(\frac{2\pi}{T}x), \sin(\frac{2\pi}{T}x))$, we can recover $x \bmod T$.*

Lemma 3.4 (FoNE preserves numeracy). *Given a number’s Fourier Number Embedding $\text{FoNE}(x)$, its integer digit length m , and the decimal digit length n , by using Lemma 3.3, we can recover $x \bmod 10^i$ for each integer i in the range $-n + 1$ to m .*

A natural question that arises here is why do we need $x \bmod 10$ when we know $x \bmod 100$. Hence, next, we show the necessity of different periods.

Lemma 3.5 (Necessity of different periods). *When T becomes very large in a circular embedding (Definition 3.1), the difference $\frac{2\pi}{T}(x + 1) - \frac{2\pi}{T}x$ approaches zero, causing the embedded representations of x and $x + 1$ to become arbitrarily close on the unit circle. Consequently, a single large T cannot sufficiently distinguish adjacent values in the embedding. Hence, one must choose T across a broad range of scales to ensure that the embedding remains adequately distinguishable for all values of x . In this paper, we choose T as 10^i , $\forall i$, so that each T effectively captures one digit of x .*

Note that since FoNE uses the ratio between entries to represent numbers, it is unaffected by layer normalization and RMS normalization (Lemma C.2), in contrast to xVal [13], which uses the magnitudes of entries.

To provide a clear illustration of our method, we present a detailed example demonstrating how we map number 4.17 to its embedding.

Example 3.6. *Consider $x = 4.17$. Its Fourier Number Embedding is given by*

$$[\phi(4.17, 0.1), \phi(4.17, 1), \phi(4.17, 10)],$$

where ϕ is defined in Definition 3.1. From these components, by using Lemma 3.3, we can recover

$$[4.17 \bmod 0.1, 4.17 \bmod 1, 4.17 \bmod 10],^1$$

which simplifies to $[0.07, 0.17, 4.17]$. If we used only $T = 10$, then $\phi(4.17, 10)$ would be nearly indistinguishable from $\phi(4.18, 10)$, causing the embedding to lose fine-grained information about less significant digits. However, with these chosen periods T , we can capture all the digits.

3.2 Decoding

As each number has its own FoNE, calculating the logits for all possible numbers becomes computationally infeasible. Therefore, we introduce a novel decoding head that maps hidden states from Fourier space to number space as shown in Figure 1(d). Below, we explicitly define the loss function and prediction function for each digit and then show how to combine these to obtain the final loss and prediction.

¹For real x and positive real m , $x \bmod m$ is defined as $x - m \cdot \lfloor \frac{x}{m} \rfloor$, yielding a value in the range $[0, m)$

Algorithm 2 Fourier Number Loss & Prediction

```
1: function FOURIERNUMBERLOSSFUNCTION( $h, y, i$ )
2:    $y_i \leftarrow$  the  $i$ -th digit of  $y$ 
3:    $a \leftarrow [h[2i], h[2i + 1]]$ 
4:    $b \leftarrow [\phi(0, 10), \phi(1, 10), \dots, \phi(9, 10)]^\top$ 
5:    $\text{logits} \leftarrow a \cdot b$ 
6:    $\text{loss} \leftarrow L_{\text{CE}}(y_i, \text{logits})$   $\triangleright$  Cross-entropy loss for digit  $i$ 
7:   return loss
8: end function
9: function FOURIERNUMBERPREDICTION( $h, i$ )  $\triangleright$  Prediction for digit  $i$ 
10:   $\text{logits} \leftarrow [h[2i], h[2i + 1]] \cdot [\phi(j, 10)]_{j=0, \dots, 9}$ 
11:   $\hat{y}_i \leftarrow \arg \max_{j \in \{0, \dots, 9\}} \text{logits}[j]$ 
12:  return  $\hat{y}_i$ 
13: end function
```

Definition 3.7 (Fourier Number Loss Function). Let $h \in \mathbb{R}^d$ denote the last-layer hidden state of the model. Let y_i denote the i -th digit of the label number y . For digit i , we define the Fourier Number Loss Function L_{FoNE} as:

$$L_{\text{FoNE}}(h, y, i) := L_{\text{CE}}\left(y_i, \underbrace{([h[2i], h[2i + 1]])}_{1 \times 2} \cdot \underbrace{\begin{bmatrix} \phi(0, 10) \\ \vdots \\ \phi(9, 10) \end{bmatrix}}_{2 \times 10}\right)$$

This construction allows each digit to be treated as a separate prediction task while sharing the same underlying model representation h . By taking the average of $L_{\text{FoNE}}(h, y, i)$ over all digit positions i , we obtain the final training loss.

Definition 3.8 (Fourier Number Prediction for the i -th digit). Let $h \in \mathbb{R}^d$ denote the last-layer hidden state of the model. For digit i , we define the Fourier Number Prediction as:

$$\hat{y}_i := \arg \max_{j \in \{0, \dots, 9\}} \left([h[2i], h[2i + 1]] \cdot [\phi(j, 10)] \right).$$

Here, \hat{y}_i is determined by the similarity between the hidden states and the circular embedding of number in $\{0, \dots, 9\}$ as illustrated in Figure 1(d). Once we have computed \hat{y}_i for each digit i , the final prediction for the entire number can be formed by concatenating these digit-wise predictions. We defer the detailed algorithms to Appendix A.

3.3 Incorporating FoNE into Input Sequences

The integration of Fourier Number Embedding (FoNE) into input sequences proceeds as follows, as illustrated in Figure 1:

1. Extract all numbers from the input sequence to create a number list. Replace each number with the token [Num] and tokenize the sequence to obtain a token list.
2. Embed the token list using standard word embedding methods.
3. Map each number in the number list to its FoNE representation using Algorithm 1, as detailed in Section 3.1.
4. Add the FoNE to the word embedding of the corresponding [Num] token.
5. Feed the combined embeddings into the model.
6. Use the model’s output embeddings to predict the next token in the sequence.

7. If the predicted token is [Num], decode the numerical value using the method described in Section 3.2, or compute the loss during training.

This procedure ensures that FoNE embeddings are seamlessly integrated into the input sequence, enabling the model to leverage both numerical and contextual information effectively.

4 Empirical Evaluation

4.1 Experiment Setting

We evaluate the performance of our proposed *Fourier Number Embedding (FoNE)* method on arithmetic tasks designed to benchmark different number embedding methods. The dataset includes tasks such as 6-digit integer addition, 6-digit decimal addition (with 3 digits after the decimal), 5-digit integer subtraction, 3-digit integer multiplication, and 4-digit integer multiplication. These tasks are curated to measure model capabilities in accurate numeric computation. All experiments were conducted using an NVIDIA A6000.

Dataset. Each example in the dataset is formatted as [operand a] [operator] [operand b]=, where the operands **a** and **b** are sampled based on the operation type. For addition and multiplication, we ensure $a \leq b$ to avoid duplication (e.g., $a + b$ and $b + a$ are treated as identical and included only once). For subtraction, we enforce $a \geq b$ to ensure non-negative results. For an x -digit operands dataset, each operand can have up to x digits. The dataset is divided into training, validation, and test subsets as shown in Table 4 in Appendix G.

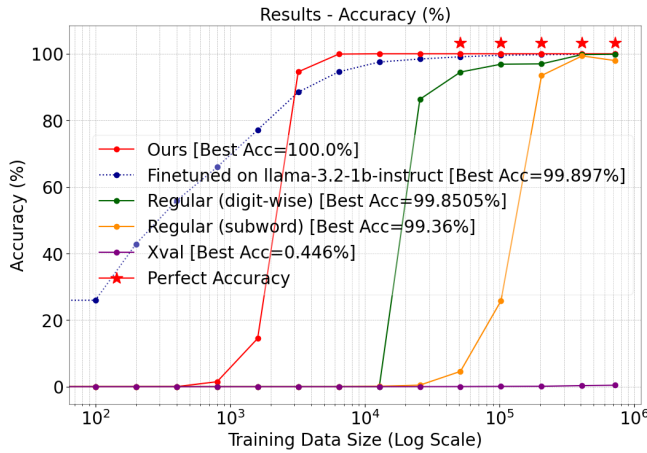
Baselines. We compare our proposed FoNE method against several baseline methods for numeric embeddings. First, we consider digit-wise tokenization, where each digit in a number is treated as an individual token. Second, we evaluate subword tokenization, where numeric values are tokenized into subword units based on the Llama3.2-1b tokenizer’s default vocabulary. Third, we include the xVAL method [13], which leverages explicit value-based representations for numeric computation. As xVAL predict floating point numbers, predictions are rounded to calculate accuracy. Finally, we fine-tune pre-trained LLMs on the same dataset for comparison.

Setup. Our experiments involve multiple configurations of transformer-based models. Specifically, we use Llama-3.2-1B-Instruct as the base model. Models were evaluated across varying sizes, ranging from small to large architectures as defined in Table 6. In Appendix H, we conduct experiments on GPT-2-Large and have the same results.

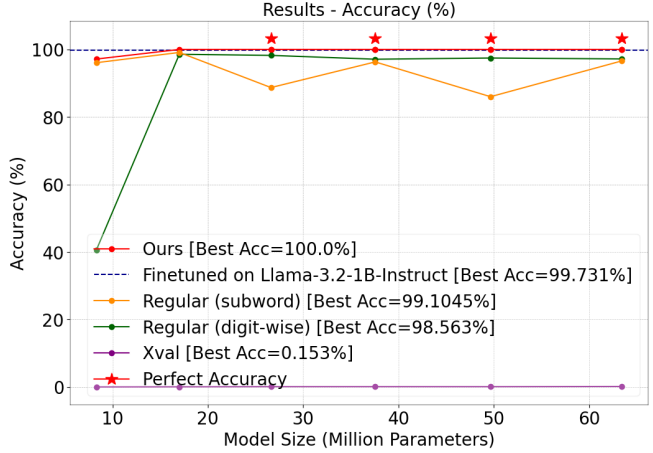
Learning rates were determined through an extensive search, with the best rates selected separately for each method based on the validation performance. Model evaluation used exact match accuracy to assess numeric prediction correctness. All models were trained from random initialization. We varied the training data size by uniformly sampling subsets and adjusted model sizes to compare accuracy across methods.

4.2 Experiment Results

Data Efficiency. Figure 2(a) illustrates the accuracy trends of different embedding methods as the data size increases for the 6-digit decimal addition task. Remarkably, our model achieves 99% accuracy with just 6,400 training samples and 37.55 million parameters, requiring $64\times$ less training data than traditional embedding methods ($409,600/6,400 = 64$). Even with only 3,200 training samples, our method outperforms the fine-tuned Llama-3.2 model. Additionally, it achieves perfect accuracy with 51,200 training samples.

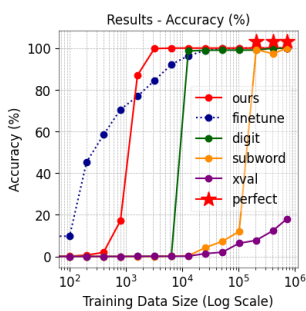


(a) 6-digit decimal addition: Acc. vs. Training Data Size

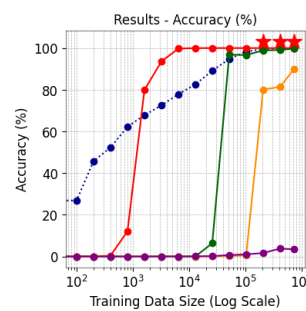
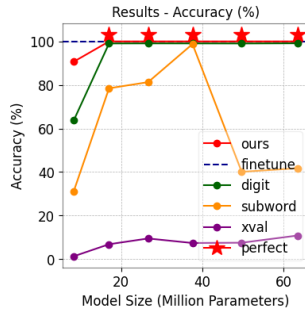


(b) 6-digit decimal addition: Acc. vs. Model Size

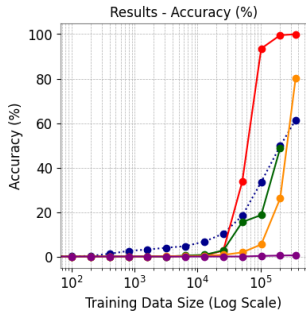
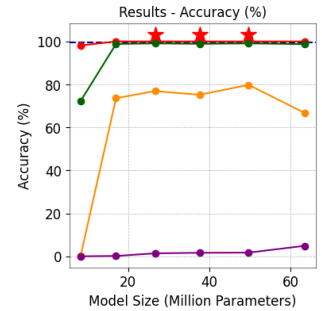
Figure 2: We train Llama-3.2-1B from scratch with random initialization using different number embedding methods on 6-digit decimal addition. The test accuracy is compared across varying data sizes and model sizes.



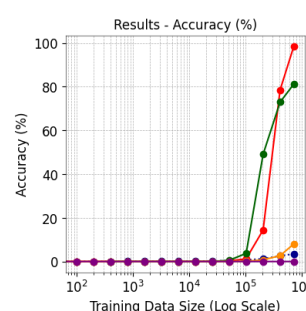
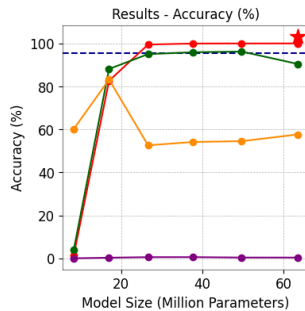
(a) 6-digit integer addition: Model&Data size vs. Acc.



(b) 5-digit integer subtraction: Model&Data size vs. Acc.



(c) 3-digit integer multiplication: Model&Data size vs. Acc.



(d) 4-digit integer multiplication: Model&Data size vs. Acc.

Figure 3: Comparison of accuracy trends for various arithmetic tasks with respect to model size and data size.

Beyond synthetic tasks, our approach also improves data efficiency in real-world scenarios. For instance, FoNE requires only 149.25 tokens on average to represent numerical values from a table in the WikiTableQuestions dataset [34], compared to 329.7 tokens used by a digit-wise tokenizer. This significant reduction in token usage highlights the efficiency of our method in encoding numerical data, making it more scalable for practical applications.

Parameter Efficiency. Figure 2(b) shows the accuracy trends of different embedding methods as the model size increases for the 6-digit decimal addition task. Our method achieves 97% accuracy with just 1 layer and 8.31 million parameters using 200k examples for training. Furthermore, with 26.62 million parameters, it surpasses the fine-tuned Llama-3.2 model and achieves 100% accuracy.

Different Tasks. We conducted the same experiments across all different datasets. As shown in Figure 3, our method consistently demonstrates superior data and parameter efficiency compared to other approaches. Notably, it is the only method that achieves perfect accuracy on 6-digit decimal addition, 6-digit integer addition, 5-digit subtraction, and 3-digit multiplication. We also show that our method performs better in a binary classification task that involves numerical values. Specifically, the task requires predicting a label based on a linear equation applied to three integers. Due to space limitations, we defer the details to Appendix B.

Training and Inference Efficiency. Table 1 compares the training and test times used for one epoch across different embedding methods. Our method is consistently faster than digit-wise and subword embedding methods, as it uses one token to embed each number. Compared with xVAL, our method consistently achieves higher accuracy. Additionally, we show the number of tokens required to tokenize the maximum number for different methods, highlighting the efficiency of our approach.

Table 1: Training and inference efficiency comparison across three arithmetic tasks. The times are reported in minutes (') and seconds (").

Method	Decimal Addition				Subtraction				Multiplication					
	Train	Time	Test	Time	Tokens	Accuracy	Train.	Test.	Toks.	Acc.	Train.	Test.	Toks.	Acc.
Ours	3'18"		29"		1	100	2'42"	29"	1	100	2'56"	33"	1	98.56
Digit-wise	11'48"		1'25"		7	99.85	9'41"	1'15"	5	99.71	10'11"	1'18"	8	81.21
Subword	6'46"		58"		3	97.94	5'47"	54"	2	91.66	6'20"	58"	3	8.05
xVAL	3'17"		27"		1	0.44	2'54"	27"	1	3.41	2'56"	26"	1	0

4.3 Ablation Studies

Linear Layer after FoNE. As discussed in Section 3.1, we evaluate the use of a linear layer applied after FoNE and compare it with the approach of appending zeros to align the embedding dimensions with the model’s input requirements. As shown in Table 2, both configurations achieve almost the same accuracy. Hence, either way can be used to align FoNE with the embedding dimension.

Table 2: Accuracy Comparison Across Datasets

Task	Linear Layer	Zero Padding
Decimal Addition	100%	100%
Integer Addition	100%	100%
Multiplication	99.95%	99.91%
Subtraction	100%	100%

Effect of Different Periods. As discussed in Section 3.1, the modular group captures the necessary information for each digit, ensuring the effectiveness of our approach. We test the model with base periods of [2, 5, 10], [5], and [7], as shown in Table 3. The [2, 5, 10] configuration achieves accuracy comparable to that of the 10-period setup across different datasets. In this paper, we choose single 10 to make it

more parameter efficient. However, configurations using only mod5 or mod7 exhibit significantly lower accuracy. This is because neither mod5 nor mod7 can fully represent the required information for all digits.

Table 3: Accuracy Comparison Across Datasets and Periods

Dataset	2,5,10	10	5	7
Decimal Addition	100	100	1.52	3.64
Integer Addition	100	100	1.55	0.02
Multiplication	99.99	99.95	3.67	1.91
Subtraction	100	100	4.64	0.24

The mispredictions are attributed to the absence of critical modular results. As illustrated in Table 7 in Appendix G, in the decimal addition task, using only a mod5 representation prevents the model from distinguishing between certain digits, such as 2 and 7, which results in errors.

Necessity of Sine and Cosine Encoding. A natural question arises: are sinusoidal encodings truly necessary for arithmetic tasks? One could directly encode each digit into a separate dimension of the embedding, representing a number like 567 as [5, 6, 7]. However, this approach fails to achieve perfect accuracy. For instance, numbers such as 999 and 888 become nearly indistinguishable after layer normalization, which reduces their differences and can lead to confusion during training. We evaluate this direct encoding method on 6-digit decimal addition and, after performing a learning rate search, find that the best accuracy is 99.3% with a learning rate of 0.01 and training for 100 epochs. In contrast, FoNE achieves better accuracy in just 6 epochs with the same dataset and model size. This suggests that naive direct encoding does not adequately preserve numerical distinctions for reliable arithmetic operations. As illustrated in Table 8 in the appendix, the model frequently mispredicts 8 as 9, further demonstrating the limitations of direct encoding in preserving numerical structure.

5 Discussion

Q1: Why do we choose components with periods that are multiples of 10, i.e., 10, 100, 1000...?

As shown in Zhou et al. [49] and Figure 8, pre-trained LLMs trained on diverse datasets and strategies consistently learn nearly identical key frequency components. These components have periods of 10 and its divisors, such as 2 and 5. Since mod 10 can already represent a single digit, we believe that mod 2 and mod 5 contribute to enhancing robustness. Models trained on real-world text data—where numbers are almost always expressed in decimal—commonly learn frequency components that correspond to mod 10. We could, in principle, choose different bases (such as 2, 16, etc.), and if the training data contained enough examples in those representations, the model might well learn those frequencies too. However, most large language models primarily encounter numbers in base 10.

Q2: How does the FoNE handle numbers with longer digit sequences?

The maximum digit length that a `float64` data type can represent is 15 digits. When x exceeds 15 digits in length, applying $\text{FoNE}(x)$ directly may result in a loss of precision. To address this, x can be divided into smaller chunks, and FoNE can be applied to each chunk independently. For example, x can be split into groups of five digits. The FoNE can then be calculated for each chunk, resulting in a representation of length 10 per chunk, as each digit is encoded in two dimensions. These embeddings are subsequently concatenated to obtain the final number embedding for x .

By using this method, as shown in Figure 4(a), an 8-layer transformer trained on 60-digit addition achieved an average accuracy of 97.42% across different operand length with just one forward pass. This demonstrates the effectiveness of FoNE in handling long sequences.

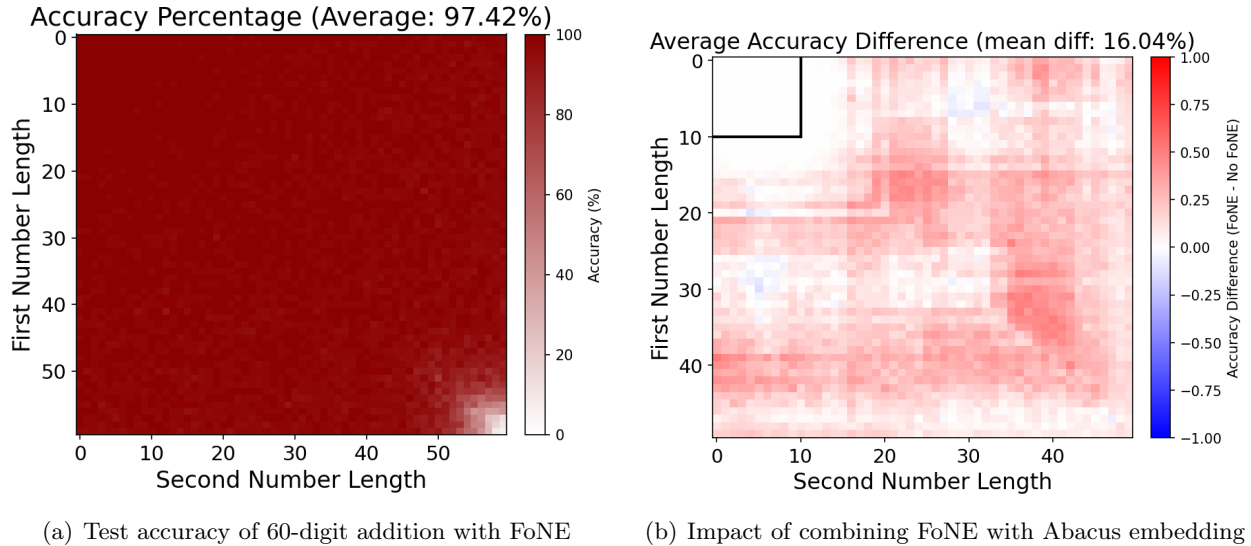


Figure 4: (a) Average accuracy of an 8-layer transformer model on 60-digit addition tasks using FoNE for chunked input. (b) Performance improvements achieved by combining FoNE with the Abacus embedding method across various random seeds. The transformer is trained on addition tasks with up to 10-digits numbers (represented by the smaller square) and tested up to 50-digit numbers.

Q3: Can FoNE combine with other positional embedding?

Yes, FoNE can be combined with other positional embedding methods. For instance, we integrated FoNE with the Abacus embedding method [24], which operates on digit-wise tokenization. In this setup, the embeddings for each digit (0–9) are replaced with their corresponding Fourier Number Embeddings.

We trained an 8-layer transformer model on integer addition tasks with up to 10 digits and tested it on addition tasks involving up to 50-digit numbers. The results, as illustrated in Figure 4(b) and Figure 10 in Appendix F, show that incorporating FoNE consistently improves the performance of the Abacus method across various random seeds. This highlights the complementary benefits of combining FoNE with other positional embedding strategies.

Q4: Will FoNE affect the semantic meaning of numbers like years?

As discussed by Meng et al. [27], the semantic meaning or memory of tokens is often inferred from the MLP layers in transformer models. Since LLMs are typically equipped with sufficient capacity, the precise numerical embedding of numbers takes precedence over encoding their semantic meanings directly within the embeddings. Moreover, as noted by Yao et al. [45], LLMs are capable of developing specialized circuits to handle different query types. Consequently, FoNE is designed to provide accurate numerical representations while allowing the model’s architecture to manage semantic contexts independently. An important future direction is the integration of FoNE with pre-trained LLMs, enabling the efficient adoption of numerical representations within existing large-scale models. This approach could enhance numerical reasoning capabilities while leveraging the extensive knowledge and contextual understanding embedded in pre-trained LLMs.

6 Conclusion

In this paper, we introduced FoNE, a novel method for representing numbers in the embedding space of LLMs. By leveraging Fourier features, FoNE directly maps numbers into a compact and precise representation, bypassing tokenization inefficiencies and preserving essential numerical properties.

FoNE has significant implications for pre-training LLMs. By incorporating FoNE, models can develop a robust understanding of numerical concepts, addressing a fundamental limitation in current

architectures. We expect this capability extends beyond simple arithmetic to support a wide range of number-related tasks, including time-series analysis, quantitative reasoning, and complex operations in fields like physics and mathematics.

By integrating FoNE into pre-training strategies, future models can overcome the limitations of existing tokenization schemes, achieve greater computational efficiency. We believe FoNE represents a significant step toward equipping LLMs with the tools necessary to tackle complex challenges with precision and rigor.

Acknowledgments

This research is supported in part by AWS credits through an Amazon Faculty research award, a NAIRR Pilot award, and Microsoft accelerating foundations research grant, and a Google Research Scholar Award. M. Soltanolkotabi is also supported by the Packard Fellowship in Science and Engineering, a Sloan Research Fellowship in Mathematics, an NSF-CAREER under award #1846369, and NSF-CIF awards #1813877 and #2008443, NSF SLES award #2417075. and NIH DP2LM014564-01. R. Jia was also supported by the National Science Foundation under Grant No. IIS-2403436. V. Sharan was supported in part by an NSF CAREER Award CCF-2239265 and an Amazon Research Award. Any opinions, findings, and conclusions or recommendations expressed in this material are those of the author(s) and do not necessarily reflect the views of the National Science Foundation. The work was done in part while some of the authors were visiting the Simons Institute for the Theory of Computing.

References

- [1] Marah Abdin, Jyoti Aneja, Hany Awadalla, Ahmed Awadallah, Ammar Ahmad Awan, Nguyen Bach, Amit Bahree, Arash Bakhtiari, Jianmin Bao, Harkirat Behl, et al. Phi-3 technical report: A highly capable language model locally on your phone. *arXiv preprint arXiv:2404.14219*, 2024.
- [2] Josh Achiam, Steven Adler, Sandhini Agarwal, Lama Ahmad, Ilge Akkaya, Florencia Leoni Aleman, Diogo Almeida, Janko Altschmidt, Sam Altman, Shyamal Anadkat, et al. Gpt-4 technical report. *arXiv preprint arXiv:2303.08774*, 2023.
- [3] Jiawang Bai, Li Yuan, Shu-Tao Xia, Shuicheng Yan, Zhifeng Li, and Wei Liu. Improving vision transformers by revisiting high-frequency components. In *European Conference on Computer Vision*, pages 1–18. Springer, 2022.
- [4] Wenhui Chen, Ming Yin, Max Ku, Pan Lu, Yixin Wan, Xueguang Ma, Jianyu Xu, Xinyi Wang, and Tony Xia. Theoremqa: A theorem-driven question answering dataset. In *Proceedings of the 2023 Conference on Empirical Methods in Natural Language Processing*, pages 7889–7901, 2023.
- [5] Karl Cobbe, Vineet Kosaraju, Mohammad Bavarian, Mark Chen, Heewoo Jun, Lukasz Kaiser, Matthias Plappert, Jerry Tworek, Jacob Hilton, Reiichiro Nakano, et al. Training verifiers to solve math word problems. *arXiv preprint arXiv:2110.14168*, 2021.
- [6] Abhimanyu Dubey, Abhinav Jauhri, Abhinav Pandey, Abhishek Kadian, Ahmad Al-Dahle, Aiesha Letman, Akhil Mathur, Alan Schelten, Amy Yang, Angela Fan, et al. The llama 3 herd of models. *arXiv preprint arXiv:2407.21783*, 2024.
- [7] Nouha Dziri, Ximing Lu, Melanie Sclar, Xiang Lorraine Li, Liwei Jiang, Bill Yuchen Lin, Sean Welleck, Peter West, Chandra Bhagavatula, Ronan Le Bras, et al. Faith and fate: Limits of transformers on compositionality. *Advances in Neural Information Processing Systems*, 36, 2024.

- [8] Xi Fang, Weijie Xu, Fiona Anting Tan, Jiani Zhang, Ziqing Hu, Yanjun Qi, Scott Nickleach, Diego Socolinsky, Srinivasan Sengamedu, and Christos Faloutsos. Large language models on tabular data—a survey. *arXiv e-prints*, pages arXiv–2402, 2024.
- [9] Guhao Feng, Kai Yang, Yuntian Gu, Xinyue Ai, Shengjie Luo, Jiacheng Sun, Di He, Zhenguo Li, and Liwei Wang. How numerical precision affects mathematical reasoning capabilities of llms. *arXiv preprint arXiv:2410.13857*, 2024.
- [10] Pierre-Étienne Fiquet and Eero Simoncelli. A polar prediction model for learning to represent visual transformations. *Advances in Neural Information Processing Systems*, 36, 2024.
- [11] Yanjun Gao, Skatje Myers, Shan Chen, Dmitriy Dligach, Timothy A Miller, Danielle Bitterman, Matthew Churpek, and Majid Afshar. When raw data prevails: Are large language model embeddings effective in numerical data representation for medical machine learning applications? *arXiv preprint arXiv:2408.11854*, 2024.
- [12] Jonas Geiping and Tom Goldstein. Cramming: Training a language model on a single gpu in one day. In *International Conference on Machine Learning*, pages 11117–11143. PMLR, 2023.
- [13] Siavash Golkar, Mariel Pettee, Michael Eickenberg, Alberto Bietti, Miles Cranmer, Geraud Krawezik, Francois Lanusse, Michael McCabe, Ruben Ohana, Liam Parker, et al. xval: A continuous number encoding for large language models. *arXiv preprint arXiv:2310.02989*, 2023.
- [14] Jiuxiang Gu, Chenyang Li, Yingyu Liang, Zhenmei Shi, Zhao Song, and Tianyi Zhou. Fourier circuits in neural networks: Unlocking the potential of large language models in mathematical reasoning and modular arithmetic. *arXiv preprint arXiv:2402.09469*, 2024.
- [15] Keji He, Chenyang Si, Zhihe Lu, Yan Huang, Liang Wang, and Xinchao Wang. Frequency-enhanced data augmentation for vision-and-language navigation. *Advances in Neural Information Processing Systems*, 36, 2024.
- [16] Albert Q Jiang, Alexandre Sablayrolles, Arthur Mensch, Chris Bamford, Devendra Singh Chaplot, Diego de las Casas, Florian Bressand, Gianna Lengyel, Guillaume Lample, Lucile Saulnier, et al. Mistral 7b. *arXiv preprint arXiv:2310.06825*, 2023.
- [17] Chengyue Jiang, Zhonglin Nian, Kaihao Guo, Shanbo Chu, Yinggong Zhao, Libin Shen, and Kewei Tu. Learning numeral embeddings. *arXiv preprint arXiv:2001.00003*, 2019.
- [18] Ming Jin, Shiyu Wang, Lintao Ma, Zhixuan Chu, James Y Zhang, Xiaoming Shi, Pin-Yu Chen, Yuxuan Liang, Yuan-Fang Li, Shirui Pan, et al. Time-llm: Time series forecasting by reprogramming large language models. *arXiv preprint arXiv:2310.01728*, 2023.
- [19] Zhijing Jin, Yuen Chen, Felix Leeb, Luigi Gresele, Ojasv Kamal, Zhiheng Lyu, Kevin Blin, Fernando Gonzalez Adauto, Max Kleiman-Weiner, Mrinmaya Sachan, et al. Cladder: A benchmark to assess causal reasoning capabilities of language models. *Advances in Neural Information Processing Systems*, 36, 2024.
- [20] Nayoung Lee, Kartik Sreenivasan, Jason D Lee, Kangwook Lee, and Dimitris Papailiopoulos. Teaching arithmetic to small transformers. *arXiv preprint arXiv:2307.03381*, 2023.
- [21] Peiyuan Liu, Hang Guo, Tao Dai, Naiqi Li, Jigang Bao, Xudong Ren, Yong Jiang, and Shu-Tao Xia. Taming pre-trained llms for generalised time series forecasting via cross-modal knowledge distillation. *arXiv preprint arXiv:2403.07300*, 2024.

- [22] Xiao Liu, Zirui Wu, Xueqing Wu, Pan Lu, Kai-Wei Chang, and Yansong Feng. Are llms capable of data-based statistical and causal reasoning? benchmarking advanced quantitative reasoning with data. *arXiv preprint arXiv:2402.17644*, 2024.
- [23] Qianli Ma, Zhen Liu, Zhenjing Zheng, Ziyang Huang, Siying Zhu, Zhongzhong Yu, and James T Kwok. A survey on time-series pre-trained models. *IEEE Transactions on Knowledge and Data Engineering*, 2024.
- [24] Sean McLeish, Arpit Bansal, Alex Stein, Neel Jain, John Kirchenbauer, Brian R Bartoldson, Bhavya Kailkhura, Abhinav Bhatele, Jonas Geiping, Avi Schwarzschild, et al. Transformers can do arithmetic with the right embeddings. *arXiv preprint arXiv:2405.17399*, 2024.
- [25] Sean McLeish, Avi Schwarzschild, and Tom Goldstein. Benchmarking chatgpt on algorithmic reasoning. *arXiv preprint arXiv:2404.03441*, 2024.
- [26] Kazem Meidani, Parshin Shojaee, Chandan K Reddy, and Amir Barati Farimani. Snip: Bridging mathematical symbolic and numeric realms with unified pre-training. *arXiv preprint arXiv:2310.02227*, 2023.
- [27] Kevin Meng, David Bau, Alex Andonian, and Yonatan Belinkov. Locating and editing factual associations in gpt. *Advances in Neural Information Processing Systems*, 35:17359–17372, 2022.
- [28] Mike A Merrill, Mingtian Tan, Vinayak Gupta, Tom Hartvigsen, and Tim Althoff. Language models still struggle to zero-shot reason about time series. *arXiv preprint arXiv:2404.11757*, 2024.
- [29] Neel Nanda, Lawrence Chan, Tom Lieberum, Jess Smith, and Jacob Steinhardt. Progress measures for grokking via mechanistic interpretability. *arXiv preprint arXiv:2301.05217*, 2023.
- [30] Rodrigo Nogueira, Zhiying Jiang, and Jimmy Lin. Investigating the limitations of transformers with simple arithmetic tasks. *arXiv preprint arXiv:2102.13019*, 2021.
- [31] Maxwell Nye, Anders Johan Andreassen, Guy Gur-Ari, Henryk Michalewski, Jacob Austin, David Bieber, David Dohan, Aitor Lewkowycz, Maarten Bosma, David Luan, et al. Show your work: Scratchpads for intermediate computation with language models. *arXiv preprint arXiv:2112.00114*, 2021.
- [32] Chris Olah, Nick Cammarata, Ludwig Schubert, Gabriel Goh, Michael Petrov, and Shan Carter. An overview of early vision in inceptionv1. *Distill*, 5(4):e00024–002, 2020.
- [33] Bruno A Olshausen and David J Field. Sparse coding with an overcomplete basis set: A strategy employed by v1? *Vision research*, 37(23):3311–3325, 1997.
- [34] Panupong Pasupat and Percy Liang. Compositional semantic parsing on semi-structured tables. In *Proceedings of the 53rd Annual Meeting of the Association for Computational Linguistics and the 7th International Joint Conference on Natural Language Processing (Volume 1: Long Papers)*, pages 1470–1480, Beijing, China, July 2015. Association for Computational Linguistics. doi: 10.3115/v1/P15-1142. URL <https://aclanthology.org/P15-1142>.
- [35] Yasaman Razeghi, Robert L Logan IV, Matt Gardner, and Sameer Singh. Impact of pretraining term frequencies on few-shot reasoning. *arXiv preprint arXiv:2202.07206*, 2022.
- [36] Maria Sahakyan, Zeyar Aung, and Talal Rahwan. Explainable artificial intelligence for tabular data: A survey. *IEEE access*, 9:135392–135422, 2021.
- [37] David Saxton, Edward Grefenstette, Felix Hill, and Pushmeet Kohli. Analysing mathematical reasoning abilities of neural models. *arXiv preprint arXiv:1904.01557*, 2019.

- [38] Ruoqi Shen, Sébastien Bubeck, Ronen Eldan, Yin Tat Lee, Yuanzhi Li, and Yi Zhang. Positional description matters for transformers arithmetic. *arXiv preprint arXiv:2311.14737*, 2023.
- [39] Jasivan Alex Sivakumar and Nafise Sadat Moosavi. How to leverage digit embeddings to represent numbers? *arXiv preprint arXiv:2407.00894*, 2024.
- [40] Dhanasekar Sundararaman, Shijing Si, Vivek Subramanian, Guoyin Wang, Devamanyu Hazarika, and Lawrence Carin. Methods for numeracy-preserving word embeddings. In *Proceedings of the 2020 Conference on Empirical Methods in Natural Language Processing (EMNLP)*, pages 4742–4753, 2020.
- [41] Mingtian Tan, Mike A Merrill, Vinayak Gupta, Tim Althoff, and Thomas Hartvigsen. Are language models actually useful for time series forecasting? *arXiv preprint arXiv:2406.16964*, 2024.
- [42] Matthew Tancik, Pratul Srinivasan, Ben Mildenhall, Sara Fridovich-Keil, Nithin Raghavan, Utkarsh Singhal, Ravi Ramamoorthi, Jonathan Barron, and Ren Ng. Fourier features let networks learn high frequency functions in low dimensional domains. *Advances in neural information processing systems*, 33:7537–7547, 2020.
- [43] Avijit Thawani, Jay Pujara, Pedro A Szekely, and Filip Ilievski. Representing numbers in nlp: a survey and a vision. *arXiv preprint arXiv:2103.13136*, 2021.
- [44] Hugo Touvron, Louis Martin, Kevin Stone, Peter Albert, Amjad Almahairi, Yasmine Babaei, Nikolay Bashlykov, Soumya Batra, Prajjwal Bhargava, Shruti Bhosale, et al. Llama 2: Open foundation and fine-tuned chat models. *arXiv preprint arXiv:2307.09288*, 2023.
- [45] Yunzhi Yao, Ningyu Zhang, Zekun Xi, Mengru Wang, Ziwen Xu, Shumin Deng, and Huajun Chen. Knowledge circuits in pretrained transformers. *arXiv preprint arXiv:2405.17969*, 2024.
- [46] Longhui Yu, Weisen Jiang, Han Shi, Jincheng Yu, Zhengying Liu, Yu Zhang, James T Kwok, Zhenguo Li, Adrian Weller, and Weiyang Liu. Metamath: Bootstrap your own mathematical questions for large language models. *arXiv preprint arXiv:2309.12284*, 2023.
- [47] Hattie Zhou, Arwen Bradley, Etai Littwin, Noam Razin, Omid Saremi, Josh Susskind, Samy Bengio, and Preetum Nakkiran. What algorithms can transformers learn? a study in length generalization. *arXiv preprint arXiv:2310.16028*, 2023.
- [48] Tian Zhou, Peisong Niu, Liang Sun, Rong Jin, et al. One fits all: Power general time series analysis by pretrained lm. *Advances in neural information processing systems*, 36:43322–43355, 2023.
- [49] Tianyi Zhou, Deqing Fu, Vatsal Sharan, and Robin Jia. Pre-trained large language models use fourier features to compute addition. *arXiv preprint arXiv:2406.03445*, 2024.
- [50] Zhejian Zhou, Jiayu Wang, Dahua Lin, and Kai Chen. Scaling behavior for large language models regarding numeral systems: An example using pythia. *arXiv preprint arXiv:2409.17391*, 2024.

Appendix

Roadmap In Appendix A, we provide the detailed algorithm for computing the final loss and making number predictions. In Appendix B, we present the results of the binary classification task. In Appendix C, we provide the preliminaries and the missing proofs from the main paper. In Appendix D, we offer additional evidence of the existence of Fourier features in pre-trained LLMs. In Appendix E, we demonstrate the ability of Transformers to solve long-sequence addition using FoNE. In Appendix F, we show how FoNE, combined with Abacus embedding, improves the results. In Appendix G, we provide additional experimental settings that were missing from the main paper. In Appendix H, we show that our method produces similar results on the GPT-2 Large model. In Appendix I, we present our method’s performance on the R^2 metric.

A Fourier Number Final Loss & Prediction

In this section, we provide the detail algorithm of how we get the final loss and final prediction as defined in Section 3.1.

Algorithm 3 Fourier Number Final Loss & Prediction

```

1: function FOURIERNUMBERFINALLOSS( $h, y, m, n$ ) ▷ Compute average loss
2:   totalLoss  $\leftarrow$  0
3:    $\mathcal{I} \leftarrow [m + n]$ 
4:   for  $i \in \mathcal{I}$  do
5:     digitLoss  $\leftarrow$  FOURIERNUMBERLOSSFUNCTION( $h, y, i$ )
6:     totalLoss  $\leftarrow$  totalLoss + digitLoss
7:   end for
8:   finalLoss  $\leftarrow$   $\frac{\text{totalLoss}}{|\mathcal{I}|}$  ▷ Average over all digit positions
9:   return finalLoss
10: end function
11: function FOURIERNUMBERFINALPREDICTION( $h, m, n$ ) ▷ Compute final prediction
12:    $\hat{y} \leftarrow 0$ 
13:    $\mathcal{I}_{\text{frac}} \leftarrow [0, \dots, n - 1]$  ▷ Fractional digit indices
14:    $\mathcal{I}_{\text{int}} \leftarrow [n, \dots, m + n - 1]$  ▷ Integer digit indices
15:   for  $i \in \mathcal{I}_{\text{frac}}$  do
16:     logits $_i \leftarrow [h[2i], h[2i + 1]] \cdot [\phi(j, 10)]_{j=0, \dots, 9}$ 
17:      $\hat{y}_i \leftarrow \arg \max_{j \in \{0, \dots, 9\}} \text{logits}_i[j]$ 
18:      $\hat{y} \leftarrow \hat{y} + \hat{y}_i \cdot 10^{-(n-i)}$  ▷ Scale fractional part by  $10^{-(n-i)}$ 
19:   end for
20:   for  $j \in \mathcal{I}_{\text{int}}$  do
21:     logits $_j \leftarrow [h[2j], h[2j + 1]] \cdot [\phi(j, 10)]_{j=0, \dots, 9}$ 
22:      $\hat{y}_j \leftarrow \arg \max_{j \in \{0, \dots, 9\}} \text{logits}_j[j]$ 
23:      $\hat{y} \leftarrow \hat{y} + \hat{y}_j \cdot 10^{j-n}$  ▷ Scale integer part by  $10^j$ 
24:   end for
25:   return  $\hat{y}$ 
26: end function

```

B FoNE on Binary Classification Task

In this section, we demonstrate that FoNE outperforms other methods on binary classification tasks, benefiting from its precise representation.

Dataset Each example in the dataset is formatted as $[\text{num1}, \text{num2}, \text{num3}]$, where the integers num1 , num2 , and num3 are sorted in ascending order ($\text{num1} \leq \text{num2} \leq \text{num3}$) to ensure uniqueness and eliminate duplicate representations of the same combination. The integers are uniformly sampled from the range $[0, 1000]$. The label for each example is determined by evaluating the linear equation

$$a \cdot \text{num1} + b \cdot \text{num2} + c \cdot \text{num3} - d,$$

using predefined coefficients $a = 1.5$, $b = -2$, $c = 0.5$, and $d = 10$ and $a = 1.5$, $b = -2$, $c = 0.5$, and $d = -190$. If the result is greater than zero, the label is assigned as 1; otherwise, it is assigned as 0. The dataset is divided into training, validation, and test subsets, as outlined in Table 4.

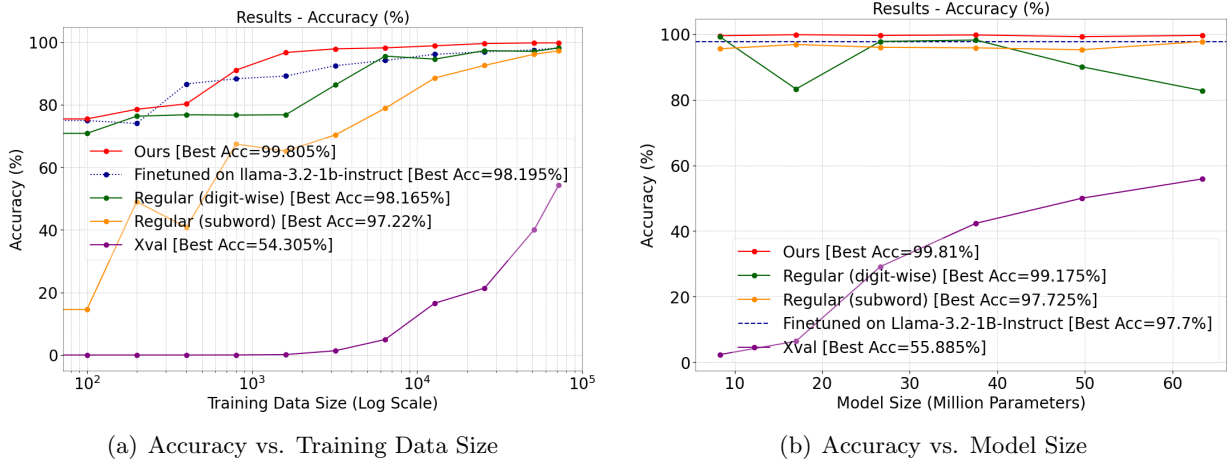


Figure 5: We train Llama-3.2-1B from scratch with random initialization using different number embedding methods on number classification where $d = 10$. The test accuracy is compared across varying data sizes and model sizes.

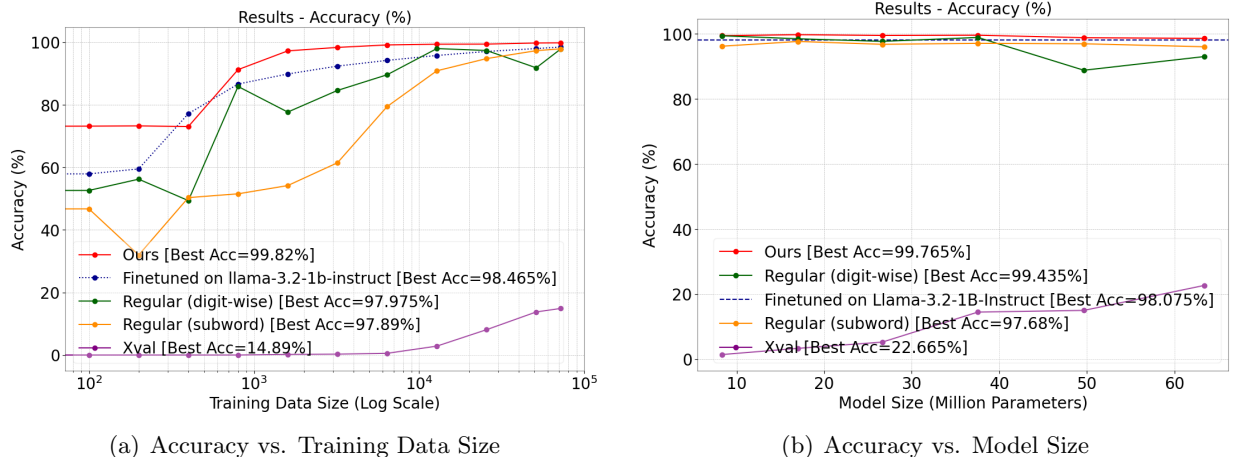


Figure 6: We train Llama-3.2-1B from scratch with random initialization using different number embedding methods on number classification where $d = -190$. The test accuracy is compared across varying data sizes and model sizes.

C Preliminaries and Missing Proof

C.1 Preliminaries

In this section, we provide the necessary mathematical definitions and concepts used throughout the paper.

Period and Frequency. A function $f(x)$ is periodic with period $T > 0$ if $f(x + T) = f(x)$ for all x . The period T represents the smallest positive value for which the function repeats. The frequency f of a periodic function is the reciprocal of its period, $f = \frac{1}{T}$, and describes the number of cycles completed in one unit interval. For the sine and cosine functions $\cos(\frac{2\pi}{T}x)$ and $\sin(\frac{2\pi}{T}x)$, the period is T .

Unit Circle. The unit circle is the set of points in the plane at a distance of 1 from the origin, given by $x^2 + y^2 = 1$. The coordinates of points on the unit circle can be parameterized as $(\cos \theta, \sin \theta)$, where θ is the angle measured counterclockwise from the positive x -axis. For any angle θ , $\cos \theta$ represents the x -coordinate, and $\sin \theta$ represents the y -coordinate.

Two-Argument Inverse Tangent. The two-argument inverse tangent function, $\text{atan2}(y, x)$, determines the angle θ (modulo 2π) given the coordinates $(x, y) = (\cos \theta, \sin \theta)$. Specifically,

$$\theta = \text{atan2}(y, x),$$

which resolves the angle θ uniquely based on the signs of x and y .

Modular Arithmetic. Modular arithmetic considers equivalence classes of numbers under a modulus $T > 0$. For integers a and b , $a \equiv b \pmod{T}$ if $T \mid (a - b)$, meaning a and b differ by an integer multiple of T .

Fourier Representation. Periodic functions with period T can be represented using the fundamental frequencies $\frac{2\pi}{T}$. For example, the embeddings $(\cos(\frac{2\pi}{T}x), \sin(\frac{2\pi}{T}x))$ capture the periodicity of x modulo T by mapping it to a unique point on the unit circle.

C.2 Missing Proof

In this section, we provide some missing proofs.

Lemma C.1 (Formal version of Lemma 3.3). *Given the pair $(\cos(\frac{2\pi}{T}x), \sin(\frac{2\pi}{T}x))$, we can recover $x \bmod T$.*

Proof. Let $\theta = \frac{2\pi}{T}x$. Then the given pair becomes

$$(\cos(\theta), \sin(\theta)).$$

From this pair, one can recover θ uniquely modulo 2π . Concretely, θ can be obtained (modulo 2π) using the two-argument inverse tangent function:

$$\theta \equiv \text{atan2}(\sin(\theta), \cos(\theta)) \pmod{2\pi}.$$

Since $\theta = \frac{2\pi}{T}x$, we have

$$x = \frac{T}{2\pi} \theta.$$

Hence x is determined up to integer multiples of T , i.e., $x \bmod T$.

In other words, if

$$(\cos(\frac{2\pi}{T}x_1), \sin(\frac{2\pi}{T}x_1)) = (\cos(\frac{2\pi}{T}x_2), \sin(\frac{2\pi}{T}x_2)),$$

then $\frac{2\pi}{T}x_1 \equiv \frac{2\pi}{T}x_2 \pmod{2\pi}$, which implies $x_1 \equiv x_2 \pmod{T}$. Therefore, from the pair $(\cos(\frac{2\pi}{T}x), \sin(\frac{2\pi}{T}x))$, we can indeed recover $x \bmod T$. \square

Lemma C.2 (Layer-Normalized FoNE Preserves Numeracy). *Given a number's Layer-Normalized Fourier Number Embedding $\text{LN}(\text{FoNE}(x) + \mathbf{p})$, where $\text{FoNE}(x)$ is the Fourier Number Embedding of x and \mathbf{p} is an orthogonal positional encoding vector, assume the mean of $\text{FoNE}(x) + \mathbf{p}$ is 0. Let m be the integer digit length of x and n be the decimal digit length of x . Then, using Lemma 3.3, we can recover $x \bmod 10^i$ for each integer i in the range $-n + 1$ to m .*

Proof. Assume the mean of $\mathbf{x} = \text{FoNE}(x) + \mathbf{p}$ is 0, i.e., $\mu = 0$. Under this assumption, LayerNorm simplifies to:

$$\text{LN}(\mathbf{x}) = \frac{\mathbf{x}}{\sigma},$$

where σ is the standard deviation of \mathbf{x} .

Let $\mathbf{u} = \text{FoNE}(x)$ encode the scalar x , and let \mathbf{p} be an orthogonal positional encoding vector such that:

$$\|\mathbf{u}\| = \|\mathbf{p}\| = 1 \quad \text{and} \quad \mathbf{u} \cdot \mathbf{p} = 0.$$

Then, the input to LayerNorm is:

$$\mathbf{x} = \mathbf{u} + \mathbf{p}.$$

The standard deviation σ of \mathbf{x} is given by:

$$\sigma = \sqrt{\frac{1}{d} \sum_{i=1}^d (\mathbf{x}_i - \mu)^2},$$

where d is the dimensionality of \mathbf{x} . Since $\mu = 0$, this simplifies to:

$$\sigma = \sqrt{\frac{1}{d} \|\mathbf{x}\|^2}.$$

Substitute $\mathbf{x} = \mathbf{u} + \mathbf{p}$:

$$\|\mathbf{x}\|^2 = \|\mathbf{u} + \mathbf{p}\|^2 = \|\mathbf{u}\|^2 + \|\mathbf{p}\|^2 + 2\mathbf{u} \cdot \mathbf{p}.$$

By orthogonality and unit norm, $\mathbf{u} \cdot \mathbf{p} = 0$, $\|\mathbf{u}\|^2 = 1$, and $\|\mathbf{p}\|^2 = 1$. Thus:

$$\|\mathbf{x}\|^2 = 1 + 1 + 0 = 2.$$

Therefore:

$$\sigma = \sqrt{\frac{1}{d} \cdot 2} = \sqrt{\frac{2}{d}}.$$

The LayerNorm operation simplifies to:

$$\text{LN}(\mathbf{x}) = \frac{\mathbf{x}}{\sigma} = \frac{\mathbf{u} + \mathbf{p}}{\sqrt{\frac{2}{d}}} = \sqrt{\frac{d}{2}}(\mathbf{u} + \mathbf{p}).$$

This rescales \mathbf{u} and \mathbf{p} by a factor of $\sqrt{\frac{d}{2}}$.

The key observation is that LayerNorm applies a **uniform scaling** to all components of \mathbf{x} . Since \mathbf{u} and \mathbf{p} are orthogonal and their relative directions are preserved, the numerical relationships encoded in \mathbf{u} (which represent x) are preserved up to a scaling factor.

By Lemma 3.3, the numeracy of x is preserved. This means we can recover $x \bmod 10^i$ for all i in the range $-n + 1 \leq i \leq m$, as the normalized embedding retains the necessary information about x . □

The same result holds for RMSNorm because it also applies a uniform scaling (based on the root mean square of the input) while preserving the relative directions of the embedding components, thus maintaining the numeracy of x .

D More evidence about Fourier features

D.1 Emergence of Fourier Features during Pre-training

We follow Zhou et al. [49] and conduct the same Fourier analysis on Pythia model. In Figure 7, we show how Pythia gradually learns the Fourier features during pre-training. With different model size, the model gradually learn the same frequency components.

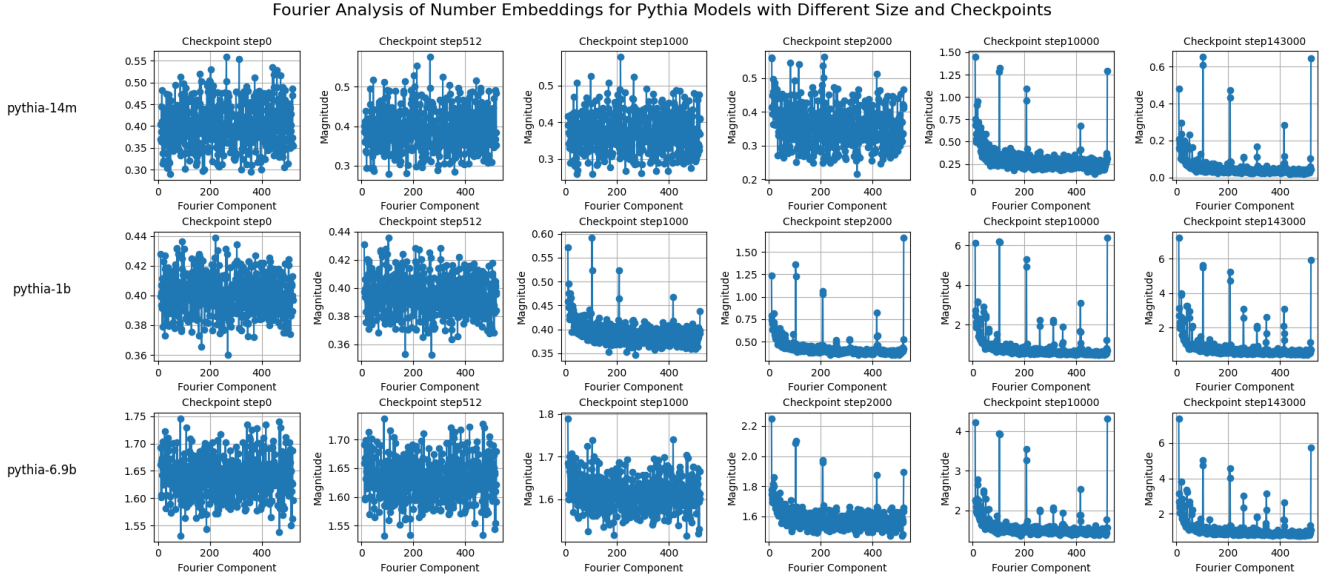


Figure 7: Fourier analysis of the Pythia model’s number embeddings across pre-training checkpoints. The figure illustrates how the Fourier features are progressively learned during pre-training, showing the emergence of specific frequency components. Models of varying sizes exhibit a similar trend, gradually learning the same frequency components over time.

We extend the work of Zhou et al. [49] to other pre-trained LLMs and observe similar findings: pre-trained LLMs, regardless of the dataset used, tend to learn the same outlier frequency components.

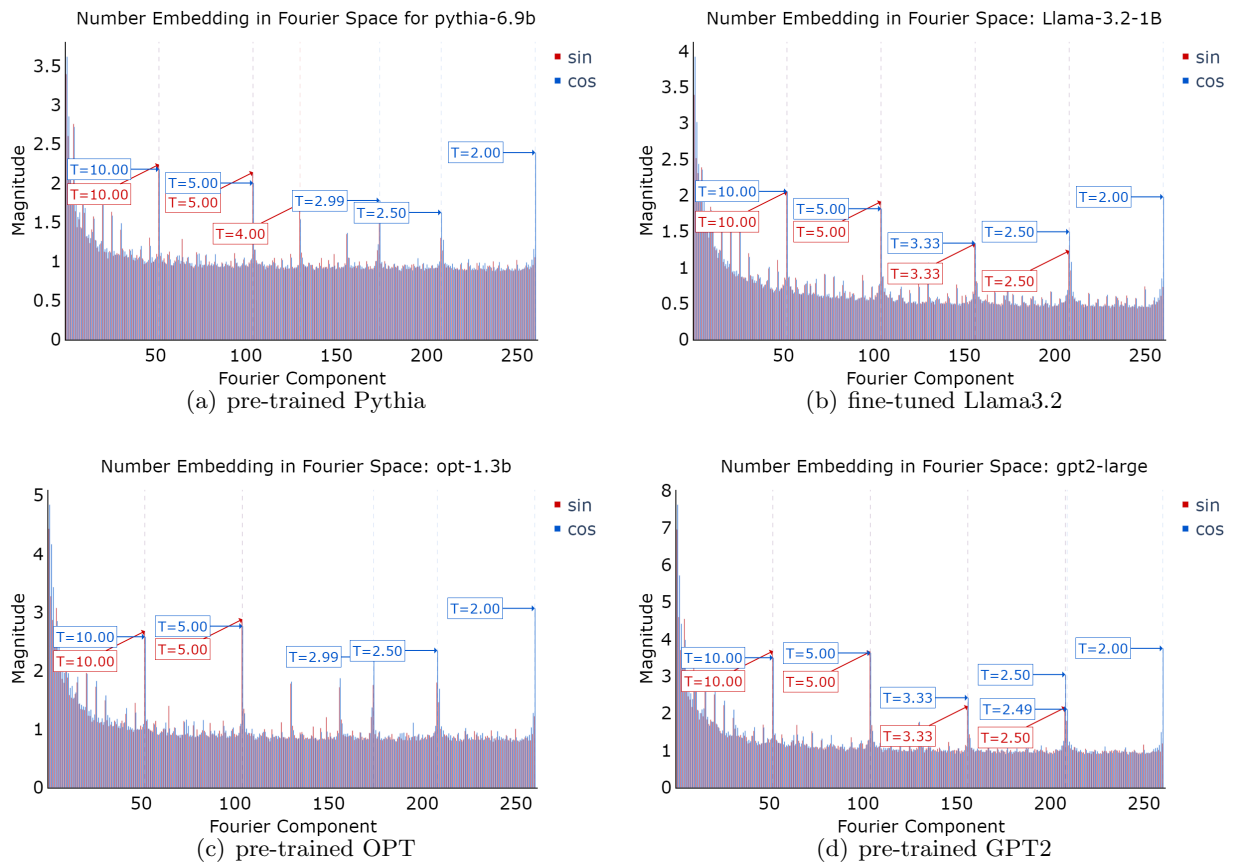


Figure 8: Number embedding in Fourier space for different pre-trained models.

E FoNE for 60-digit Integer Addition in One Forward Pass

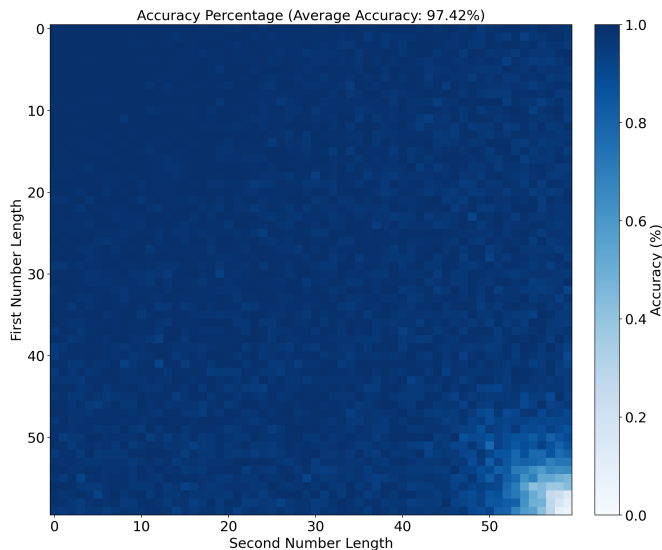


Figure 9: Accuracy of an 8-layer transformer on 60-digit addition tasks, illustrating the effectiveness of FoNE embeddings in handling long sequences. The model achieves an average accuracy of 97.42% across different operand lengths, showcasing its capability in numerical precision and sequence representation.

As discussed in Section 5, the maximum digit length that a `float64` data type can precisely represent is 15 digits. Consequently, even if we convert numbers to `float64` and then back to `float16` to match the model weight precision it still introduce numerical inaccuracies when the input x exceeds 15 digits. To mitigate this issue, we process x by dividing it into smaller chunks, allowing the FoNE to operate effectively without precision loss.

Specifically, x is split into groups of five digits, and FoNE is applied independently to each chunk. Each digit within a chunk is encoded into two dimensions, resulting in an embedding of length 10 per chunk. These chunk embeddings are then concatenated to form the final representation of x . This method ensures that even for long inputs, the FoNE still preserve the numeracy of the numbers.

We adopt the data generation approach from [24], which includes all combinations of operand lengths (i, j) up to a maximum length k , generating 20 million stratified samples to ensure balanced representation across all length pairs. Training is conducted using a language model cramming approach [12], constrained to 8 exaFLOP (equivalent to 24 hours of training on a single Nvidia RTX A6000 GPU). Using this strategy, as depicted in Figure 4(a), an 8-layer transformer trained on 60-digit addition achieves an average accuracy of 97.42% across various operand lengths in just one forward pass. This result underscores the effectiveness of the FoNE in processing long numbers with high precision and computational efficiency in just one forward pass.

F Combine FoNE with Abacus

We train decoder-only causal language models to solve arithmetic problems, following the setup described in McLeish et al. [24]. Inputs are formatted in a least-significant-digit-first order (e.g., $98282 + 3859172 = 2787472$), without padding between digits or operands. The training dataset includes all combinations of operand lengths (i, j) up to a maximum length k , with 20 million stratified samples ensuring balanced representation across all length pairs.

For input representation, we combine Fourier Number Embeddings (FoNE) with the Abacus method [24]. That each digit is embedded with FoNE. Training is conducted using a language model cramming

approach [12], constrained to 8 exaFLOP (equivalent to 24 hours of training on a single Nvidia RTX A6000 GPU).

We train and evaluate the models across three runs, each with a different random seed, as shown in Figure 10. Results indicate that incorporating FoNE enables the Abacus method to achieve better generalization and higher accuracy.

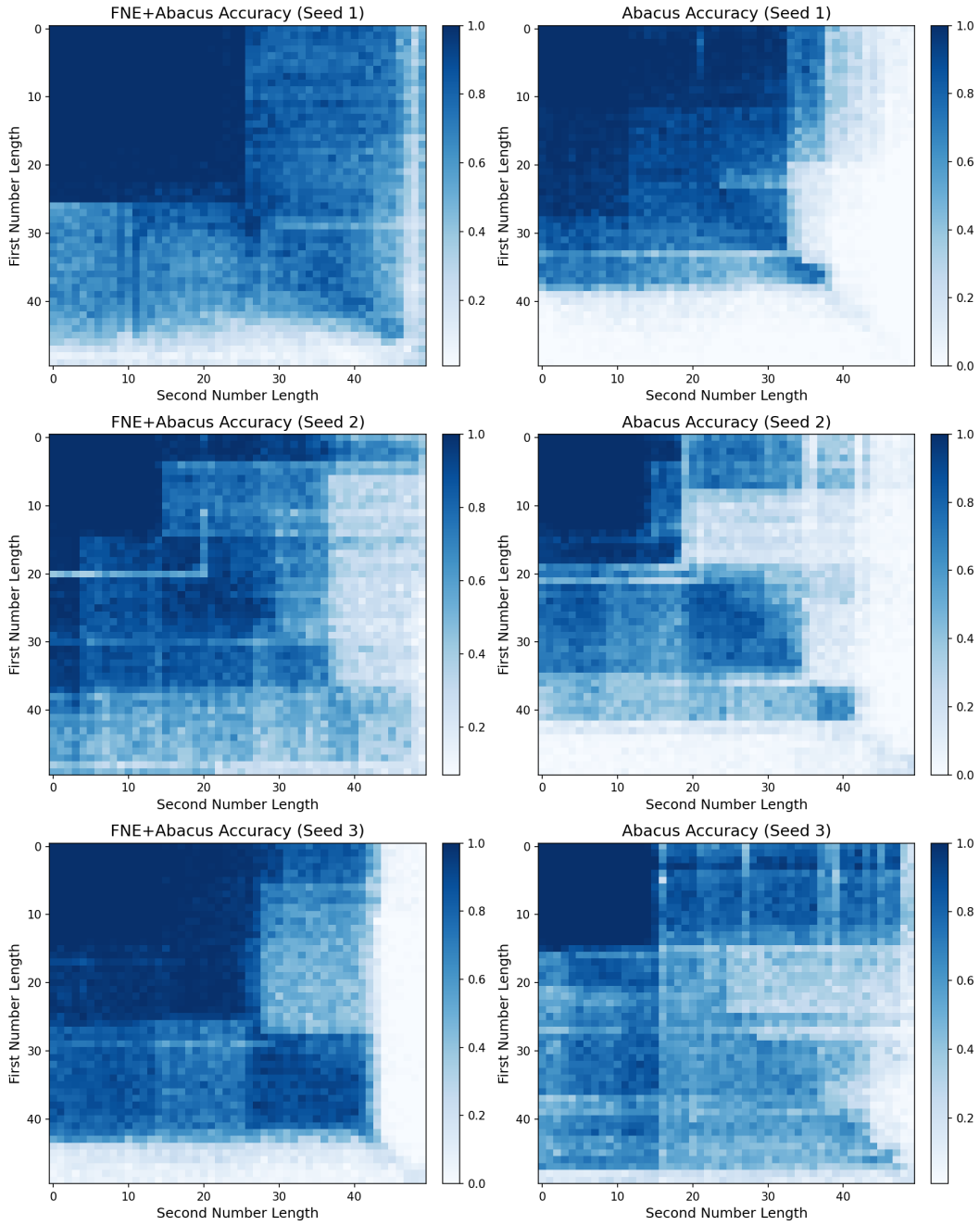


Figure 10: Heatmaps of accuracy percentages for “FoNE+Abacus” (left column) and “Abacus” (right column) across three different random seeds. Each heatmap represents accuracy as a function of the first and second number lengths, with lighter blue shades indicating higher accuracy. The color scale ranges from white (low accuracy) to blue (high accuracy). These visualizations highlight FoNE can combine with Abacus to improve performance.

G Experiment Setting

In this section, we provide the experiments settings that we used in the Section 4.1.

Learning rates were determined through an extensive search, with the best rates selected separately for each method based on validation performance. Final training hyperparameters include a learning rate of 0.005 for regular and FoNE methods, and 0.0001 for the xVal method, a batch size of 512, and 100 epochs.

Dataset	Train Size	Validation Size	Test Size
6-digit decimal addition	720,000	80,000	200,000
6-digit integer addition	720,000	80,000	200,000
5-digit integer subtract	720,000	80,000	200,000
3-digit integer multiplication	360,000	40,000	100,000
4-digit integer multiplication	720,000	80,000	200,000
classification	720,00	80,00	200,00

Table 4: Dataset Sizes for Training, Testing, and Validation

Dataset	Model Size for Varying Data Size	Data Size for Varying Model Size
6-digit decimal addition	37.55M	200,000
6-digit integer addition	37.55M	200,000
5-digit integer subtract	37.55M	200,000
3-digit integer multiplication	37.55M	360,000
4-digit integer multiplication	37.55M	360,000
4-digit integer multiplication	37.55M	360,000
classification	37.55M	50,000

Table 5: Dataset and Configuration Sizes for Model and Data Variation Experiments

Model	Hidden Size	Intermediate Size	# Hidden Layers	# Attention Heads	# Key-Value Heads
1	64	256	1	4	2
2	128	512	2	4	2
3	192	768	3	6	3
4	256	1024	4	8	4
5	320	1280	5	8	4
6	384	1536	6	8	4

Table 6: Model Configuration Table

G.1 Ablation Study

In this section, we present the mispredictions of the model trained with an FoNE, where the periods are multiples of 5 instead of 10. Table 7 demonstrates that, for each digit, the mispredictions consistently deviate from the true labels by 5.

We also present the model’s mispredictions in Table 8, where each digit is encoded into a separate dimension of the embedding. For example, the number 567 is represented as [5, 6, 7]. During training, we compute the RMSE loss between the last hidden states and the labels. During prediction, we interpret each entry in the last hidden state as a single digit.

Table 7: Mispredictions in the Final Evaluation with when we embed each digit with only mod5.

Index	Predicted Value	Actual Value
1	934.03	934.585
2	3.009	558.509
3	912.311	917.366
4	6201.003	1756.008
5	1240.34	1290.84

Table 8: Mispredictions in the Final Evaluation when directly encoding numbers into their embeddings.

Index	Predicted Value	Actual Value
1	883.888	993.999
2	787.878	898.989
3	888.758	989.759
4	748.785	849.895
5	677.677	688.788
10	1179.488	1189.499

H Similar Results on GPT2-Large Based Experiments

We conduct the same experiments on decimal addition using a GPT-2 Large-based model. The results indicate that changing the model architecture does not affect the outcomes. For instance, GPT-2 Large employs LayerNorm, while Llama 3.2 uses RMSNorm.

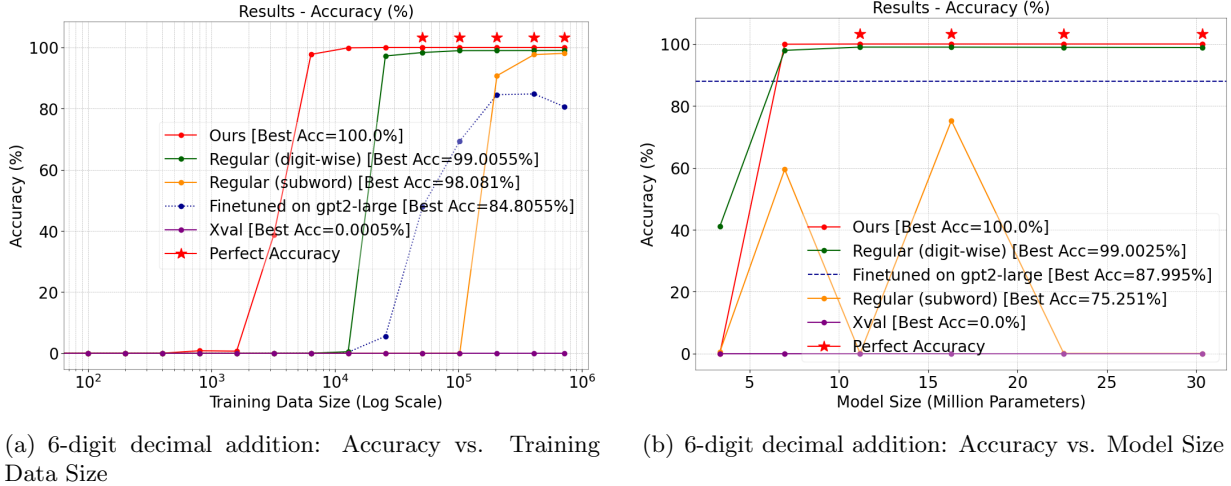


Figure 11: We train GPT2-Large from scratch with random initialization using different number embedding methods on 6-digit decimal addition. The test accuracy is compared across varying data sizes and model sizes.

I R^2 comparison

xVal [13] performs well on the R^2 metric

$$R^2 = 1 - \frac{\sum_{i=1}^n (y_i - \hat{y}_i)^2}{\sum_{i=1}^n (y_i - \bar{y})^2},$$

because it uses RMSE as its loss function. However, we demonstrate that FoNE outperforms xVal on R^2 in most tasks. We show the final R^2 on test dataset in our experiments(Section 4.2).

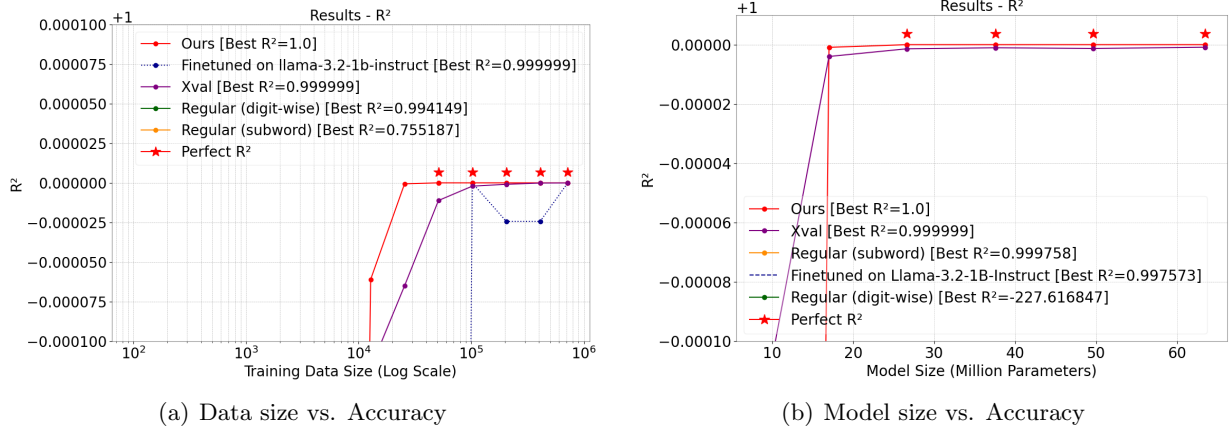


Figure 12: Comparison of R^2 trends for 6-digit decimal addition with respect to model size and data size.

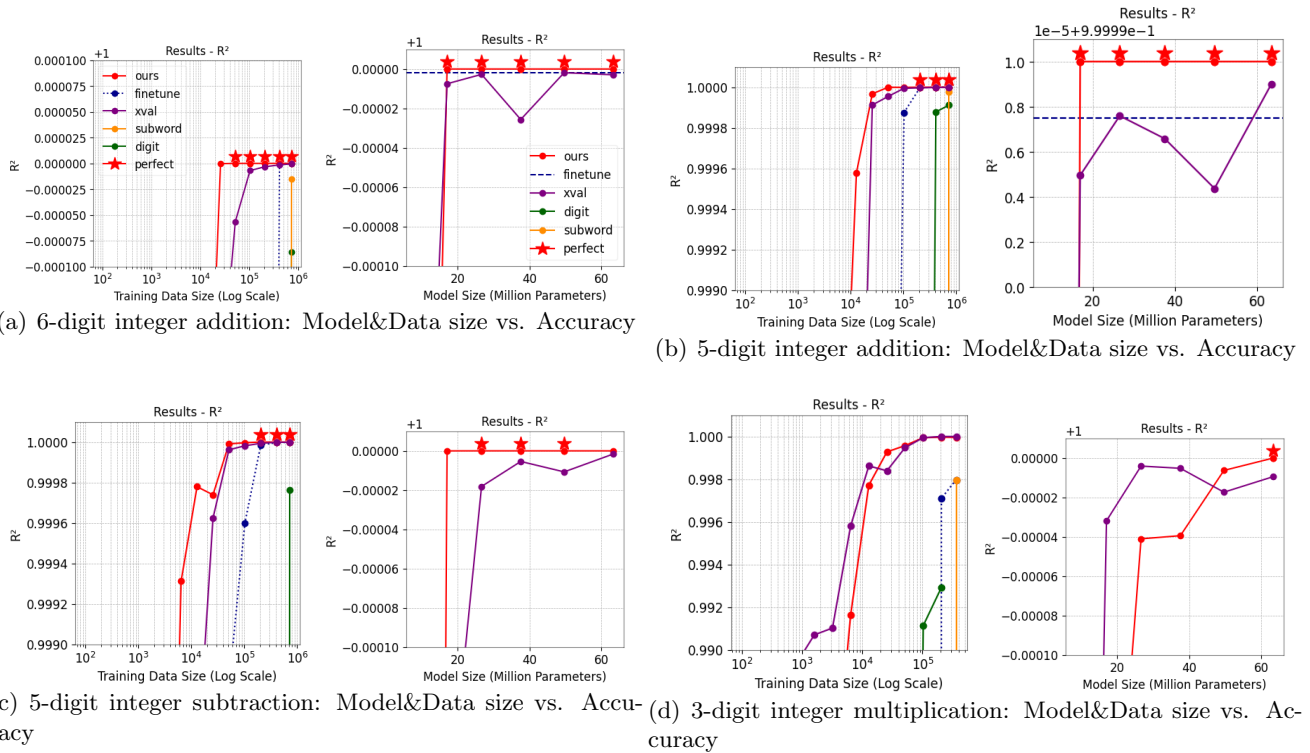


Figure 13: Comparison of R^2 trends for various arithmetic tasks with respect to model size and data size.